Quantum dynamics of the dissociation of H_2 on Rh(111)

Arezoo Dianat, Sung Sakong, and Axel Groß

*Physik-Department T30, Technische Universität München, D-85747 Garching, Germany**

(Dated: December 27, 2004)

The dissociative adsorption of H_2 on Rh(111) has been studied by high-dimensional quantum calculations using a coupled channel scheme. The potential energy surface was derived from *ab initio* total energy calculations using density functional theory together with the generalized gradient approximation to describe exchange-correlation effects. Experimentally, at high kinetic energy a step in the dissociative adsorption probability as a function of kinetic energy has been observed [M. Beutl *et al.*, Surf. Sci. **429**, 71 (1999)] which has been attributed to the opening up of new adsorption channel. This feature in the dissociation probability is reproduced in the calculations but it is not related to the opening up of an additional dissociation channel. Instead, it is caused by purely dynamical effects. In addition, rotational effects in the H_2 dissociation are addressed.

I. INTRODUCTION

The dissociation of hydrogen on low-index transition metal surfaces has been one of the model systems for the investigation of molecule-surface interactions [1–6]. It has been studied in great detail both experimentally [7–18] as well as theoretically [19–37]. Because of the light mass of H_2, quantum effects in the dissociation dynamics are important. On the other hand, recoil effects of the metal substrate can usually be neglected because of the large mass mismatch. Therefore the H_2 dissociation dynamics on metals can be described within a six-dimensional configuration space including just all molecular degrees of freedom.

Full-dimensional quantum dynamical simulations have been performed for the hydrogen dissociation on the low-index (100), (111) and (110) surfaces of various metals [20–22, 25, 31, 33–35]. These calculations are still computationally demanding and only possible if the irreducible representations of the symmetry group of the molecule-surface system are taken into account [21, 38]. In order to get a realistic potential energy surface (PES), usually first-principles total-energy calculations are performed using density functional theory together with the generalized gradient approximation (GGA) to describe exchange-correlation effects. A continuous representation of the PES is then obtained by using some appropriate and accurate interpolation scheme [39–41]

The dynamical studies indicate that the adsorption dynamics depend sensitively on the initial conditions of the impinging molecules such as the incident beam energy, the ro-vibrational quantum states and the angle of incidence. As far as adsorption systems with non-activated dissociation paths are concerned, molecular beam experiments as well as quantum dynamical studies for non-activated adsorption systems found that the sticking probability under normal incidence first decreases with energy at low kinetic energies, and then increases at higher kinetic energies [7, 12, 20, 23, 29–33, 36, 37, 42–44]. It is now well accepted that this behavior is a consequence of the corrugation and anisotropy of the multidimensional PES which leads to strong forces acting at the molecules upon adsorption. At low kinetic energies, these forces can either steer the molecule into a favorable configuration for direct dissociation [20, 36] or lead to the conversion of perpendicular kinetic energy into parallel kinetic energy and/or internal energy of the molecule so that they become temporarily dynamically trapped [29–32, 37, 45]. Both effects result in high adsorption probabilities at low kinetic energies but become suppressed at higher kinetic energies which causes the decrease in the adsorption probabilities. At even higher kinetic energies, molecules start to directly overcome the dissociation barriers.

Molecular beam experiments have shown that the adsorption probability of H_2/Rh(111) as a function of the kinetic energy of the hydrogen molecules shows the characteristics of non-activated adsorption systems [46]: first there is an decrease which is relatively small, and then the adsorption probability rises again. However, at higher kinetic energies, a peculiar feature was observed in the adsorption probability. There is a steplike structure at a kinetic energy of 450 meV which was reached for D_2 molecules seeded in a H_2 beam. This step has been attributed to the opening up of a new dissociation channel at this energy due to an additional activation barrier for dissociation in one particular area of the surface unit cell [46].

In order to analyze this step in the sticking probability, the dissociative adsorption of H_2 on Rh(111) has been studied in this work. The potential energy surface has been obtained from GGA-DFT total-energy calculations using the Vienna *ab initio* package simulation (VASP) [47, 48]. On the *ab initio*-derived PES quantum dynamical simulations have been performed by solving the time-independent Schrödinger equation in a coupled-channel scheme within the concept of the local reflection

---

*New address: Abteilung Theoretische Chemie, Universität Ulm, D- 89069 Ulm, Germany

(LORE) matrix [49]. The step-like feature is in fact reproduced in our calculations, however, there is no additional dissociation channel in the PES at higher energies. Hence the step must be caused by purely dynamical effects. Furthermore, we have also analysed rotational effects in the dissociation dynamics obtaining rotational hindering at low kinetic energies in agreement with the experiment [46].

This paper is structured as follows. In the next section, computational details for the construction of the potential energy surface and for the quantum dynamical simulations will be given. We will then present and discuss the results of our quantum dynamical calculations for the dissociation of $H_2/Rh(111)$. The paper will end with some concluding remarks.

II. COMPUTATIONAL DETAILS

A. Construction of the potential energy surface

In order to perform the quantum dynamical simulation, a continuous representation of the multidimensional potential energy surface is needed. As usual, two approximations are made. First, the Born-Oppenheimer approximation is used to decouple the motion of the electrons from the nuclear motion, restricting the reaction to take place on the electronic ground state PES only. Second, the energy exchange with the surface through phonons is neglected because of the large mass mismatch between hydrogen and the substrate metal atoms.

The PES has been mapped out by performing DFT calculations using the Vienna *ab initio* simulation package (VASP) [47]. The exchange-correlation effects have been described within the generalized gradient approximation (GGA) using the Perdew-Wang (PW-91) functional [50]. The ionic cores are represented by ultrasoft pseudopotentials [51] as constructed by G. Kresse and J. Hafner [52]. A cut-off energy of 250 eV has been found to be sufficient for converged results, but results requiring high accuracy have been checked with a 350 eV cut-off. The calculated equilibrium lattice constant, $a_{Rh} = 3.85$ Å, agrees to within 1.3% with the experimental value of 3.80 Å.

The Rh(111) surface is modeled by a slab of five layers for the (111) surface separated by 12 Å of vacuum. The energetics of hydrogen adsorption have been determined using (2×2) surface unit cells for all considered surface terminations. The two uppermost layers of the slabs have been fully relaxed. For a (2×2) surface unit cell, we used a Monkhorst-Pack **k** point set[53] of $7 \times 7 \times 1$, corresponding to 16 **k** points in the irreducible Brillouin zone, together with a first-order Methfessel-Paxton smearing[54] of width $\sigma = 0.2$ eV. All reported total energies were extrapolated to $\sigma \rightarrow 0$ eV.

For a fixed substrate, the PES of H_2 interacting with Rh(111) is six-dimensional corresponding to the six H_2 degrees of freedom. As usual, we have analysed the mul-
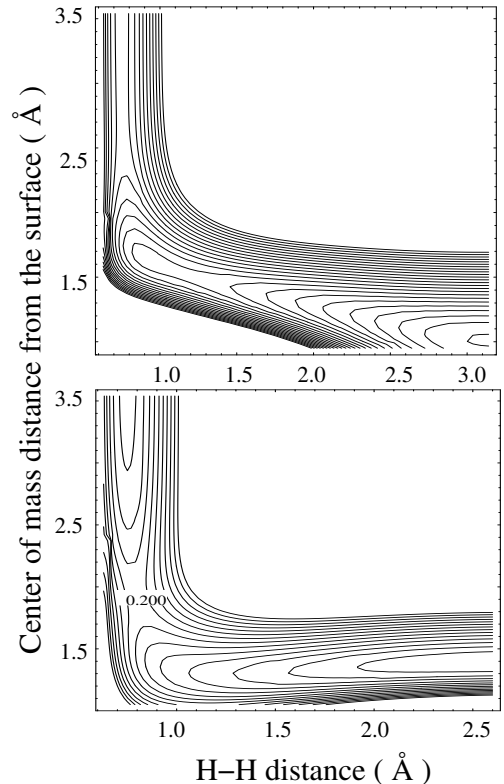

FIG. 1: Two-dimensional elbow plot of the potential energy surface determined by DFT calculations as a function of the interatomic H-H distance and the distance of the center of mass from the surface with the molecular axis being parallel to the surface. For the upper panel, the molecular center of mass is above a top site, and for the lower panel, it is located above the threefold fcc hollow site. The contour spacing is 0.15 eV.

tidimensional PES in terms of two-dimensional so-called elbow plots as a function of the interatomic H-H distance and the distance of the center of mass from the surface. In total, seven different elbow plots for the H_2 molecule above high-symmetry points of the surface unit cell have been determined, five for the molecular axis being parallel to the surface and two for a perpendicular orientation. There are non-activated paths to dissociative adsorption, but the majority of dissociation paths for fixed lateral center of mass coordinates and molecular orientation are hindered by barriers. Figure 1 shows two such elbow plots derived from a discrete set of DFT-GGA calculations for the molecular axis kept parallel to the surface and the center of mass located above the top and the threefold fcc hollow site, respectively. While the first pathway is purely attractive, the second dissociation path is hindered by a barrier of about 0.2 eV. It is obvious that the barrier for dissociative adsorption is located before the curved region of the reaction path, i.e. it is a so-called early barrier [2]. In fact, all calculated activated dissociations paths exhibit early barriers. Since these early barriers are located rather far

from the surface, they hardly show any dependence on the azimuthal orientation of the hydrogen molecule. The azimuthal variation of the barrier is less than 5 meV. Because of this small variation one can safely assume that the part of the PES crucial for the dissociation dynamics is azimuthally flat.

The quantum dynamics of the H_2 dissociative adsorption on Rh(111) has been evaluated within a coupled-channel scheme (see below) in which the H_2 wave function perpendicular to the reaction path coordinate is expanded in a suitable basis set. Usually, one chooses the curvelinear coordinate along one minimum energy path of an elbow plot as the reaction path coordinate s; the coordinate perpendicular to the reaction path is denoted by ρ. The remaining degrees of freedom are represented by two lateral center of mass coordinates X and Y and the polar and azimuthal orientation θ and ϕ of the molecule, respectively.

In order to perform the quantum dynamical calculation, a continuous representation of the *ab initio* PES is needed. We have used a parametrization which is adapted to the symmetry of the H_2/surface system. Because of the negligible dependence of the PES on the azimuthal orientation of the H_2 molecule, the relevant PES is only five-dimensional. The chosen analytical form of the 5D PES is given by

$$
\begin{aligned}
V^{corr} &= V_1^{(c)}(s) \\
&+ V_2^{(c)}(s)\big[\cos GX + \cos GY + \cos(GX + GY)\big] \\
&+ V_3^{(c)}\big[\cos 2GX + \cos 2GY + \cos(2GX + 2GY)\big] \\
V^{rot} &= V_1^{(r)}(s)\big[\cos GX + \cos GY + \cos(GX + GY)\big] \\
&\quad \cos^2\theta + V_2^{(r)}(s)\big[\cos(2GX + GY) \\
&+ \cos(2GY + GX) + \cos(GX - GY)\big]\sin^2\theta \\
V^{vib} &= \frac{\mu}{2}\omega^2(s)\rho^2.
\end{aligned}
\tag{1}
$$

where $G = 2\pi/a$ is the length of the basis vectors of the hexagonal surface reciprocal lattice, a is the nearest neighbor distance between the Rh atoms and $\omega(s)$ is the frequency of the vibrations perpendicular to the reaction path coordinate s. The unit vectors associated with the lateral coordinates $X = a(1,0)$ and $Y = a(1/2,\sqrt{3}/2)$ are nonorthogonal.

In Fig. 2 two parameterized elbow plots for both an activated and a non-activated pathway are shown which should be compared to the corresponding original DFT elbow plots presented in Fig. 1. Six *ab initio* pathways determined at high-symmetry points for parallel and perpendicular orientations of the H_2 molecule have been used in the parametrization. In the interpolation, we have particularly focused on the accurate fitting of the transition state regions where the difference between the *ab initio* results and the parameterized potential is smaller than 25 meV. On the average, however, the root mean square error of the parametrization along the minimum energy paths of the elbow plots is about 50 meV.
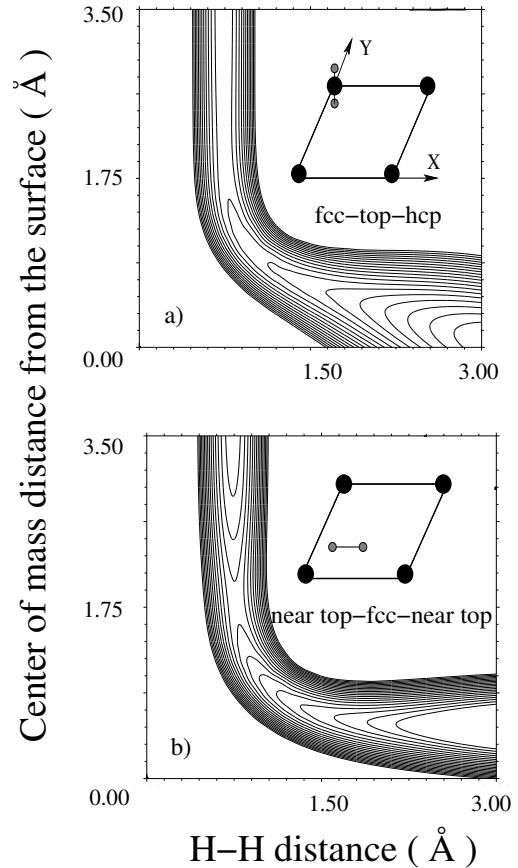

FIG. 2: Contour plots of 2D-cuts through the PES for the dissociative adsorption of H_2/Rh(111) with the molecular axis being parallel to the surface for a) a non-activated and b) an activated pathway. The lateral configrations of the hydrogen molecule which are illustrated in the inset are the same as in Fig. 1. Contour lines are drawn at intervals of 0.15 eV.

B. Quantum dynamical simulations

The quantum dynamical calculations are performed using the concept of the *local reflection* (LORE) matrix [49]. The construction of the appropriate Hamiltonian is described in detail in Ref. [21] for the H_2 interaction with a (100) surface. The hexagonal (111) surface is spanned by non-orthogonal unit vectors which introduces additional terms in the kinetic operator. The Hamiltonian is then given by

$$
\begin{aligned}
H_{5D} &= -\frac{\hbar^2}{2\mu}\left(\eta^{-1}\frac{\partial}{\partial s}\eta^{-1}\frac{\partial}{\partial s} + \eta^{-1}\frac{\partial}{\partial \rho}\eta\frac{\partial}{\partial \rho} + \frac{\mathbf{L}^2}{r_e^2}\right) \\
&- \frac{\hbar^2}{2M\sin^2\gamma}\left(\frac{\partial^2}{\partial X^2} - 2\cos\gamma\frac{\partial}{\partial X}\frac{\partial}{\partial Y} + \frac{\partial^2}{\partial Y^2}\right) \\
&+ V_{5D}(X,Y,s,\rho,\theta),
\end{aligned}
\tag{2}
$$

where M and μ are the total and reduced mass of H_2, respectively, and γ is the angle between the X and Y

axes which is $\gamma = 60°$ for a fcc(111) surface. The coupling parameter η is defined by $\eta = 1 - \kappa(s)$, where $\kappa(s)$ is the curvature of the minimum reaction path. $\vec{L}$ is the angular momentum operator, r_e the H_2 minimum energy bond length which is a function of the reaction path coordinate s. The 5D interaction potential is given by a linear combination of the appropriate potential terms in Eq. 1. In fact, the Hamiltonian describes the motion of a hydrogen molecule in all six degrees of freedom on an azimuthally flat surface. Practically this means that the azimuthal rotational quantum number m is conserved during the molecule-surface interactions.

In any coupled-channel scheme, the computational effort can be significantly reduced if the symmetry properties of the system are taken into account. Hence the hydrogen wave function has been expanded in a set of symmetry adapted wave function. In this specific study, we are mainly interested in the dissociation probability of H_2 molecules under normal incidence on the Rh(111) surface which has the C_{6v} point group symmetry. In principle, a fcc(111) surface has only a C_{3v} symmetry because of the difference between fcc and hcp three-fold hollow sites, but this difference is negligible as far as the H_2/Rh(111) interaction potential is concerned.

Since the molecule-surface potential is independent of the azimuthal angle ϕ, we need to include only parallel translational wavefunctions which are totally symmetric under C_{6v} symmetry in the case of normal incidence. The quantum numbers associated with the basis set are rotational quantum numbers up to $j_{max} = 8$, vibrational quantum number up to $v_{max} = 2$, and parallel momentum quantum numbers up to $p_{max} = 8\hbar G$, respectively. The convergence of the results with respect to the basis set has been carefully checked.

III. RESULTS AND DISCUSSIONS

In the experiments, the sticking probability of H_2 and D_2 on Rh(111) have been determined in molecular beam experiments as a function of the kinetic energy under normal incidence [46]. These experimental results are shown in Fig. 3. Kinetic energies above 0.4 eV can only been achieved by seeding techniques. Hence the experimental results for kinetic energies above 0.4 eV have been measured for D_2 seeded in H_2. However, since no isotope effect in the sticking probability for kinetic energies between 0.2 eV and 0.4 eV has been observed, it is justified to assume that also at higher energies there is no difference between the D_2 and H_2 sticking probabilities. At low kinetic energies, the sticking probability first decreases slightly and then rises again. This behavior is charateristic for non-activated adsorption systems where the sticking at small energies is dominated by steering [20, 55] and dynamical trapping processes [29–32, 37]. The most striking feature in the measured sticking probability is the bump at about 450 meV. This bump has been attributed to the opening up of an additional
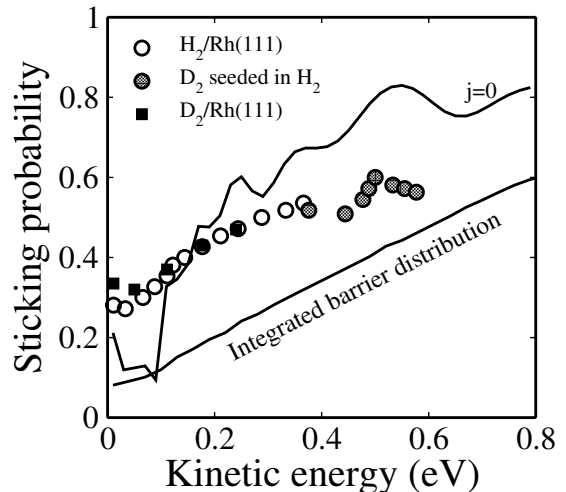

FIG. 3: Calculated quantum sticking probability versus kinetic energy under normal incidence in the ro-vibrational ground state and integrated barrier distribution based on the classical sudden approximation. The experimental result is for H_2/Rh(111) up to 450 meV and for energies larger than 450 meV D_2 is seeded in H_2.

dissociation channel in the potential energy surface at this energy [46].

The calculated sticking probability of H_2/Rh(111) for molecules initially in the rotational ground state ($j = 0$) is also included in Fig. 3. It should be mentioned that we have convoluted all our sticking results with a Gaussion function corresponding to a velocity spread of $\Delta v_i/v_i = 0.05$ in order to mimic the experimental situation of the molecular beams which have a similar velocity spread [7]. First of all we note that the calculated results agree semi-quantitatively with the experiment. At low kinetic energies, the sticking probability initially decreases, but to a larger extent than in the experiment. Still, the initial decrease is much less pronounced than in other non-activated adsorption systems [11]. We attribute this to the fact that H_2/Rh(111) is an early barrier system so that the molecules reach the barriers before they can be steered to favorable dissociation pathways or become dynamically trapped.

There is some structure in the quantum results, but most interestingly, at 450 meV there is also a pronounced bump in the calculated sticking probability. However, this bump is not associated with any additional dissociation channel. We made a careful search for such a channel in the potential energy surface, but could not find any. This is reflected in the integrated barrier distribution $P_b(E)$ which is also plotted in Fig. 3. This distribution $P_b(E)$ is the fraction of the configuration space for which the barrier towards dissociation is less than E, which corresponds to the sticking probability in the classical sudden approximation or the so-called hole-

model [56]. $P_b(E)$ is defined as

$$P_b(E) = \frac{1}{2\pi A} \int \Theta(E - E_b(\theta, \phi, X, Y)) \cos\theta d\theta d\phi dX dY, \tag{3}$$

where X, Y, θ and ϕ are the lateral and orientational coordinates of the molecule and A is the area of the surface unit cell. The function Θ is the Heavyside step function. E_b is the minimum energy barrier along a two-dimensional cut through the six-dimensional space. The integrated barrier distribution does not show any structure, in particular not at 450 meV, which indicates that at this energy there are no additional dissociation channels. Thus the occurence of the bump must be of an entirely dynamical origin.

The fact that the sticking probability is much larger than integrated barrier distribution for almost all considered kinetic energies up to 0.8 eV indicates that even at higher kinetic energies the steering forces of the potential energy surface are operative. Similar results have also been found for the system $H_2/S(2\times2)/Pd(100)$ which, however, is an activated system with a minimum energy barrier towards dissociation of 0.09 eV [22, 57]. For this system, the steering becomes less efficient at a kinetic energy of about 0.4 eV [58]. It might well be that for $H_2/Rh(111)$ the topology of the PES leads to efficient steering and enhanced dissociation at about 450 meV which then becomes suppressed above 500 meV.

It should be noted here that the parametrization of the PES is based on DFT results which have been obtained for the H_2 molecule situated above high-symmetry points of the surface unit cell. In between this high-symmetry points the parametrized PES represents an interpolation which might be erroneous. Hence we cannot rule out that indeed there could be an additional dissociation channel at about 450 meV which is responsible for the occurence of the bump in the sticking probability. Still we consider such a scenario to be rather unrealistic since usually the high-symmetry points correspond to extrema in the multidimensional PES.

We have also considered the dependence of the sticking probability on the initial rotational state of the impinging H_2 molecules. The corresponding results are shown in Fig. 4, characterized by the rotational and azimuthal quantum number j and m, respectively. In the experiments, it was found that additional rotational motion leads to a reduction of the sticking probabilities [46]. As far as the rotational motion of the molecule is concerned, the orientation of the rotational axis plays an important role. Molecules rotating in the so-called cartwheel fashion, i.e. with $m = 0$, have their molecular axis oriented preferentially perpendicular to the surface which is very unfavorable for dissociation. These molecules experience rotational hindering (see Fig. 4a), i.e., their sticking probability is suppressed with respect to non-rotating molecules. It should be noted that the presence of a bump in the sticking probability is not restricted to the non-rotating molecule. It is also reproduced for the molecules which rotate in the cartwheel fashion.
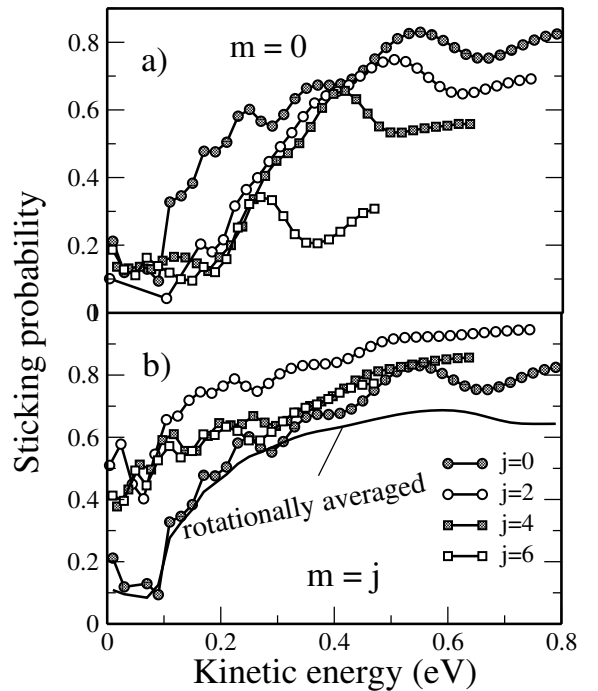

FIG. 4: Calculated sticking probability versus kinetic energy under normal incidence for different initial rotational conditions. a) Molecules initially rotating in the cartwheel fashion, i.e., with $m = 0$; b) molecules initially rotating in the helicopter fashion, i.e., with $m = j$, where j and m are the rotational and the azimuthal quantum number, respectively.

On the other hand, molecules rotating in the helicopter fashion have their molecular axis preferentially oriented parallel to the surface which is favorable for dissociation. And indeed, for the helicopter molecules, additional rotational motion enhances the sticking probability compared to non-rotating molecules, as Fig. 4b demonstrates. This behavior is well-known from other $H_2/$metal systems [20, 23, 26, 33]. Interestingly enough, however, the dependence of the sticking probability on the rotational quantum number j exhibits a non-monotonic behavior. The maximum rotational enhancement is found for $j = 2$, for larger rotational quantum numbers the enhancement becomes weaker. This is a surprising result considering the fact that the PES is azimuthally flat. Usually, the rotational enhancement increases for helicopter molecules with rising $j = m$ [20, 23, 26, 33] since for higher j values the molecular orientation becomes more and more parallel to the surface. However, this rotational enhancement is additionally mediated by an adiabatic energy transfer from the rotational motion to translation because of the extension of the intermolecular bond upon dissociation [23, 24]. This mechanism is absent in the system $H_2/Rh(111)$ because the *early* barriers are located at the beginning of the reaction zone so that the barriers suppress the dissociation before the molecules start to extend.
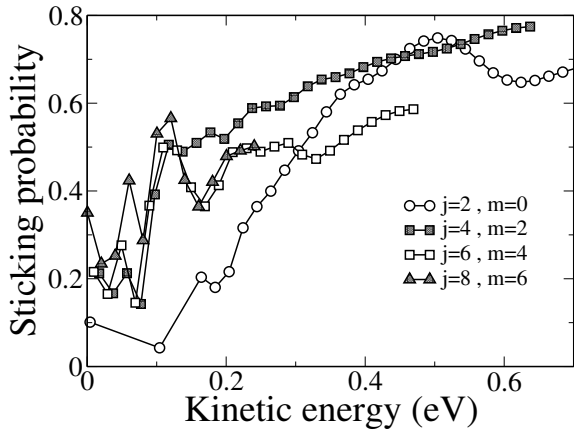
FIG. 5: Calculated sticking probability versus kinetic energy under normal incidence for H_2 molecules initially rotating in the rotational states (j, m) with $m = j - 2$, where j and m are the rotational and the azimuthal quantum number, respectively.

Since the PES is azimuthally flat, we have in addition to $\Delta j = \pm 2$ the selection rule $\Delta m = 0$ for the allowed transition between the H_2 rotational states. This means that for helicopter molecules with $m = j$ which also experience the polar anisotropy of the PES only rotational transitions with $\Delta j = +2$ are possible, i.e. there are no rotational transitions possible for these molecules which could lead to a rotational-to-translational energy transfer. Furthermore, the energetic difference between rotational states increases with increasing rotational quantum number j which means that the rotational transitions require more energy transfer from the translation for higher j values. Together, these effects lead to a reduction in the quantum transmission probability through the barrier region of H_2 helicopter molecules for increasing rotational quantum number j and thus to the non-monotonic behavior observed in Fig. 4b.

This explanation is supported by the results for the molecules initially rotating with a azimuthal quantum number $m = j - 2$ which are shown in Fig. 5. For these molecules which become more and more helicopter-like with increasing rotational quantum number j, translational-to-rotational energy transfer associated with $\Delta j = -2$ transitions is possible. And indeed, at low kinetic energies up to 0.15 eV the sticking probability rises monotonically with the rotational quantum number j up to $j = 8$; for higher kinetic energies there is some non-monotonic behavior, but much less pronounced than for the helicopter states with $m = j$.

In the experiments, the molecular beams do not correspond to molecules in one particular quantum state but rather to a statistical distribution over many states. The mean energy in the internal degrees of freedom, vibrations and rotations, is often characterized by a vibrational and rotational temperature, respectively. The rotational temperature in hydrogen beams has been esti-

mated to be 80% of the nozzle temperature of the molecular beam apparatus, but there are many uncertainties associated with the number [12, 15]. In addition, the quantum statistics of the hydrogen molecules has to be taken into account. Depending on the parallel or antiparallel coupling of the nuclear spins of the H_2 molecules one distinguishes between ortho-hydrogen and para-hydrogen. Normal of n-hydrogen corresponds to a mixture of 75% ortho-hydrogen (parallel spins, odd rotational quantum numbers) with 25% para hydrogen (antiparallel spins, even rotational quantum numbers) according to the degeneracy of the spin states (triplet and singlet).

In order to estimate the general influence of rotations on the dissociation, we have determined rotational averaged sticking probabilities for n-hydrogen which are also included in Fig. 4b. These results are obtained by performing a Boltzmann summation independently for para- and ortho-hydrogen, i.e., for even and odd rotational quantum number; thus we have taken into account the distinction between para- and ortho- hydrogen for the rotationally averaged simulation. We find that these rotational results lie below the $j = 0$ results for all considered kinetic energies, i.e., on the average additional rotations lead to a suppression of the sticking probability. Correspondingly, invoking the principle of microscopic reversibility we have also found so-called rotational cooling in the time-reverse process of adsorption, namely desorption, i.e. the mean rotational energy of desorbing molecules is less than what one would expect in thermal equilibrium. This findings are in agreement with the measurements [46]. By using seeding techniques with heavier atoms, rotational hot hydrogen beams have been produced in the experiments, i.e. molecular beams that have a higher rotational energy than non-seeded beams with the same kinetic energy. These rotationally hot beams have a reduced sticking probability compared to the non-seeded beams thus demonstrating rotational hindering.

It should be noted that the rotational averaged results do not exhibit any bump in the sticking probability around 450 meV. However, the true rotational distribution in the molecular beams is rather uncertain. Furthermore, the bump is experimentally observed for D_2 seeded in H_2 which introduces additional uncertainties about the rotational states of the molecular beams.

The dependence of the H_2 dissociation probability on the orientation of the molecules is hard to observe experimentally because it is not possible to align the nonpolar H_2 molecules in the molecular beam. However, in desorption a property can be measured which is directly related to the preferential orientation of rotating molecules, namely the rotational alignment $A_0^{(2)}$ [13, 17, 59]. It is defined as the quadrupole moment of the orientational distribution of desorbing molecules

$$A_0^{(2)} = \left\langle \frac{3m^2 - j^2}{j^2} \right\rangle . \tag{4}$$

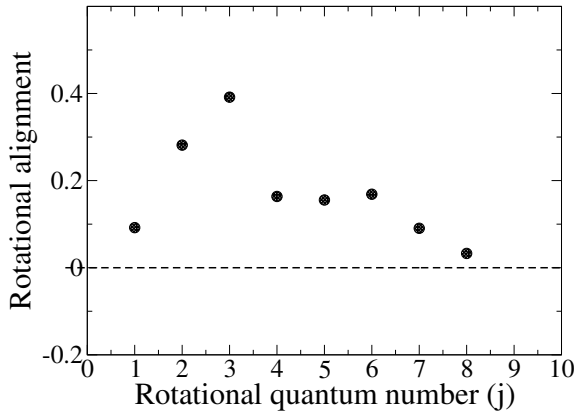A negative alignment parameter $A_0^{(2)}(j) < 0$ indicates

FIG. 6: Calculated rotational alignment in the desorption of H_2 from Rh(111) as a function of the rotational quantum number for a surface temperature of $T = 700$ K.

molecules rotating preferentially in the cartwheel fashion while $A_0^{(2)}(j) > 0$ corresponds to molecules rotating preferentially in the helicopter fashion. Unfortunately, for the system H_2/Rh(111) the rotational alignment has not been measured yet. We are still reporting our predictions for the rotational alignment in Fig. 6 which have been derived from the calculated sticking probabilities using the principle of microscopic reversibility [14, 23].

The rotational alignment parameters are all positive reflecting the fact that the parallel orientation of the molecule (helicopter molecule) is favorable for dissociation. Still they exhibit a non-monotonic behavior as a function of the rotational quantum number j. This is a direct consequence of the non-monotonic dependence of the sticking probability for helicopter molecules on j which reduces the difference in the sticking probabilities between cartwheel and helicopter molecules (see Fig. 4) and thus also the rotational alignment in desorption for high j values.

IV. CONCLUSIONS

The dissociation dynamics of H_2 on Rh(111) has been studied by solving the time-independent Schrödinger equation within a coupled-channel scheme. The potential energy surface was derived from *ab initio* total energy calculations using density functional theory (DFT) within the generalized gradient approximation (GGA) for the exchange-correlation functional. The system H_2/Rh(111) is characterized by a coexistence of activated and non-activated paths towards dissociative adsorption. At the position of the energetic barriers hindering dissociation, the intermolecular H-H bond is not significantly extended, i.e. the system is an early barrier system, which has important consequences on the dissociation dynamics.

Due to the early barriers the steering forces of the potential energy surfaces are not very effective at small kinetic energies leading only to a small enhancement of the sticking probability due to steering and dynamic trapping in the low-energy regime. The observed bump in the sticking probability at higher kinetic energies is reproduced in the calculations. It is, however, not caused by the opening up of a new dissociation channel but rather due to dynamic effects. Because of the early location of the dissociation barriers, there is almost no dependence of these barriers on the azimuthal orientation of the molecules. Consequently, molecules rotating in the helicopter fashion show an enhanced dissociation probability because of their favorable orientation. Still, the sticking probability exhibits a non-monotonic behavior for helicopter molecules as a function of the rotational quantum number due to quantum effects which is also reflected in the rotational alignment of desorbing molecules. The overall effect of rotations averaged over all orientations is to suppress the sticking probability; consequently, rotational cooling is observed in desorption.

[1] A. Groß, Surf. Sci. Rep. **32**, 291 (1998).
[2] G. R. Darling and S. Holloway, Rep. Prog. Phys. **58**, 1595 (1995).
[3] G.-J. Kroes, Prog. Surf. Sci. **60**, 1 (1999).
[4] G.-J. Kroes, A. Groß, E. J. Baerends, M. Scheffler, and D. A. McCormack, Acc. Chem. Res. **35**, 193 (2002).
[5] K. Christmann, Surf. Sci. Rep. **9**, 1 (1988).
[6] A. Groß, in *The Chemical Physics of Solid Surfaces*, edited by D. P. Woodruff (Elsevier, Amsterdam, 2003), vol. 11, chap. 1.
[7] K. D. Rendulic, G. Anger, and A. Winkler, Surf. Sci. **208**, 404 (1989).
[8] H. A. Michelsen and D. J. Auerbach, J. Chem. Phys. **94**, 7502 (1991).
[9] C. T. Rettner, D. J. Auerbach, and H. A. Michelsen, Phys. Rev. Lett. **68**, 1164 (1992).
[10] A. Hodgson, J. Moryl, P. Traversaro, and H. Zhao, Nature **356**, 501 (1992).
[11] K. D. Rendulic and A. Winkler, Surf. Sci. **299/300**, 261 (1994).
[12] M. Beutl, M. Riedler, and K. D. Rendulic, Chem. Phys. Lett. **247**, 249 (1995).
[13] D. Wetzig, R. Dopheide, M. Rutkowski, R. David, and H. Zacharias, Phys. Rev. Lett. **76**, 463 (1996).
[14] D. Wetzig, M. Rutkowski, H. Zacharias, and A. Groß, Phys. Rev. B **63**, 205412 (2001).
[15] M. Beutl, M. Riedler, and K. D. Rendulic, Chem. Phys. Lett. **256**, 33 (1996).
[16] M. Gostein and G. O. Sitz, J. Chem. Phys. **106**, 7378 (1997).
[17] H. Hou, S. J. Gulding, C. T. Rettner, A. M. Wodtke, and D. J. Auerbach, Science **277**, 80 (1997).
[18] T. Mitsui, M. K. Rose, E. Fomin, D. F. Ogletree, and M. Salmeron, Nature **422**, 705 (2003).
[19] A. Groß, B. Hammer, M. Scheffler, and W. Brenig, Phys. Rev. Lett. **73**, 3121 (1994).

[20] A. Groß, S. Wilke, and M. Scheffler, Phys. Rev. Lett. **75**, 2718 (1995).

[21] A. Groß and M. Scheffler, Phys. Rev. B **57**, 2493 (1998).

[22] A. Groß and M. Scheffler, Phys. Rev. B **61**, 8425 (2000).

[23] A. Dianat and A. Groß, Phys. Chem. Chem. Phys. **4**, 4126 (2002).

[24] G. R. Darling and S. Holloway, J. Chem. Phys. **101**, 3268 (1994).

[25] G.-J. Kroes, E. J. Baerends, and R. C. Mowrey, Phys. Rev. Lett. **78**, 3583 (1997).

[26] A. Eichler, J. Hafner, A. Groß, and M. Scheffler, Phys. Rev. B **59**, 13297 (1999).

[27] W. Diño, H. Kasai, and A. Okiji, Prog. Surf. Sci. **63**, 63 (2000).

[28] Y. Miura, H. Kasai, and W. Diño, J. Phys.: Condens. Matter **14**, L479 (2002).

[29] H. F. Busnengo, W. Dong, and A. Salin, Chem. Phys. Lett. **320**, 328 (2000).

[30] C. Crespos, H. F. Busnengo, W. Dong, and A. Salin, J. Chem. Phys. **114**, 10954 (2001).

[31] H. F. Busnengo, E. Pijper, M. F. Somers, G. J. Kroes, A. Salin, R. A. Olsen, D. Lemoine, and W. Dong, Chem. Phys. Lett. **356**, 515 (2002).

[32] M. A. Di Cesare, H. F. Busnengo, W. Dong, and A. Salin, J. Chem. Phys. **118**, 11226 (2003).

[33] A. Dianat and A. Groß, J. Chem. Phys. **120**, 5339 (2004).

[34] J. Dai and J. C. Light, J. Chem. Phys. **107**, 1676 (1997).

[35] M. F. Somers, D. A. McCormack, G.-J. Kroes, R. A. Olsen, E. J. Baerends, and R. C. Mowrey, J. Chem. Phys. **117**, 6673 (2002).

[36] M. Kay, G. R. Darling, S. Holloway, J. A. White, and D. M. Bird, Chem. Phys. Lett. **245**, 311 (1995).

[37] A. Groß and M. Scheffler, J. Vac. Sci. Technol. A **15**, 1624 (1997).

[38] G.-J. Kroes, J. G. Snijders, and R. C. Mowrey, J. Chem. Phys. **103**, 5121 (1995).

[39] H. F. Busnengo, A. Salin, and W. Dong, J. Chem. Phys. **112**, 7641 (2000).

[40] C. Crespos, M. A. Collins, E. Pijper, and G.-J. Kroes, Chem. Phys. Lett. **376**, 566 (2003).

[41] S. Lorenz, A. Groß, and M. Scheffler, to be published.

[42] A. Groß and M. Scherffler, Phys. Rev. Lett. **77**, 405 (1996).

[43] A. Groß, S. Wilke, and M. Scheffler, Surf. Sci. **357/358**, 614 (1996).

[44] A. Groß and M. Scheffler, Prog. Surf. Sci. **53**, 187 (1996).

[45] A. Groß, A. Eichler, J. Hafner, M. J. Mehl, and D. A. Papaconstantopoulos, Surf. Sci. **539**, L542 (2003).

[46] M. Beutl, J. Lensnik, and K. D. Rendulic, Surf. Sci. **429**, 71 (1999).

[47] G. Kresse and J. Furthmüller, Phys. Rev. B **54**, 11169 (1996).

[48] G. Kresse and J. Furthmüller, Comput. Mater. Sci. **6**, 15 (1996).

[49] W. Brenig, T. Brunner, A. Groß, and R. Russ, Z. Phys. B **93**, 91 (1993).

[50] J. P. Perdew, J. A. Chevary, S. H. Vosko, K. A. Jackson, M. R. Pederson, D. J. Singh, and C. Fiolhais, Phys. Rev. B **46**, 6671 (1992).

[51] D. Vanderbilt, Phys. Rev. B **41**, 7892 (1990).

[52] G. Kresse and J. Hafner, J. Phys.: Condens. Matter **6**, 8245 (1994).

[53] H. J. Monkhorst and J. D. Pack, Phys. Rev. B **13**, 5188 (1976).

[54] M. Methfessel and A. T. Paxton, Phys. Rev. B **40**, 3616 (1989).

[55] A. Groß, J. Chem. Phys. **102**, 5045 (1995).

[56] M. Karikorpi, S. Holloway, N. Henriksen, and J. K. Nørskov, Surf. Sci. **179**, L41 (1987).

[57] C. M. Wei, A. Groß, and M. Scheffler, Phys. Rev. B **57**, 15572 (1998).

[58] A. Groß, phys. stat. sol. (b) **217**, 389 (2000).

[59] D. Wetzig, M. Rutkowski, R. Etterich, W. David, and H. Zacharias, Surf. Sci. **402**, 232 (1998).